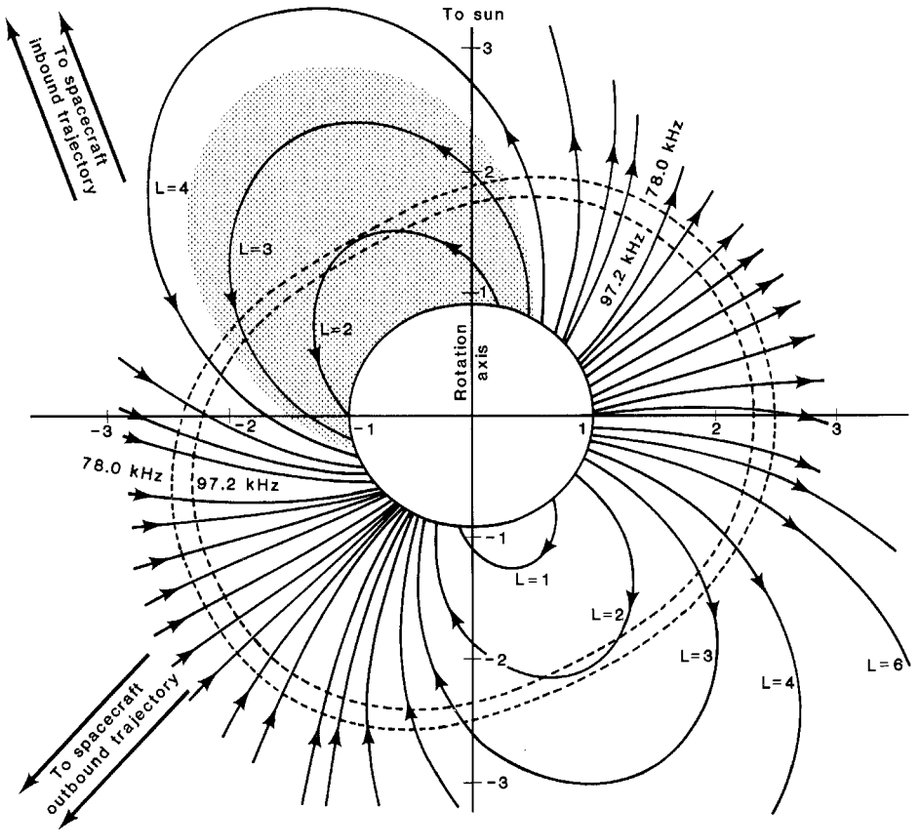

Fig. 6. The meridian plane containing the Uranian rotation axis (the vertical axis of the figure) and magnetic dipole. Dipole lines of force, with L-shell designations, and the inferred lobelike plasmasphere (stippled region) are shown.

cubic centimeter, but the radiation at both 78.0 and 58.8 kHz is generated close to the same point in space and yet escapes. A rough estimate of the plasma density gradient is possible. The height difference between the 78.0- and 97.2-kHz gyro emission surfaces is about 0.2 R_U in the region of interest. In one possible source region this radial height projects (on the plane perpendicular to the line of sight) to a much smaller value, perhaps about 0.05 R_U, over which the density declines to $(78/97)^2$ or 0.65 of its value at the position where the 97.2-kHz radiation was blocked. This decline, if it were to continue linearly, would produce a zero-density plasma within 0.15 R_U. Outside this L shell, the plasma density was so low that even 58.2-kHz radiation was scarcely affected. The corresponding plasma density is therefore much less than 42 electrons per cubic centimeter.

A sharply defined plasma cloud, called the plasmasphere, surrounds Earth (*5*). Earth's plasmapause is controlled by a dawn-to-dusk electric field across the magnetosphere and its tail. By analogy, we would expect that plasma outside the Uranian plasmasphere moves under control of convecting tubes of magnetic force. These tubes ultimately would interact with the magnetospheric boundary. The plasma inside the Uranian plasmasphere would be controlled by the planet's rotation. The crossover region from external to internal control would, according to this expectation, create the sharp plasmapause that we may have detected.

REFERENCES AND NOTES

1. J. W. Warwick, J. B. Pearce, R. G. Peltzer, A. C. Riddle, *Space Sci. Rev.* **21**, 309 (1977).
2. D. A. Gurnett and C. K. Goertz, *J. Geophys. Res.* **86**, 717 (1981).
3. J. W. Warwick *et al.*, *Science* **215**, 582 (1982).
4. N. F. Ness *et al.*, *ibid.* **233**, 85 (1986).
5. D. P. Stern and N. F. Ness, *Annu. Rev. Astron. Astrophys.* **20**, 139 (1982).

28 March 1986; accepted 5 May 1986

First Plasma Wave Observations at Uranus

D. A. GURNETT, W. S. KURTH, F. L. SCARF, R. L. POYNTER

Radio emissions from Uranus were detected by the Voyager 2 plasma wave instrument about 5 days before closest approach at frequencies of 31.1 and 56.2 kilohertz. About 10 hours before closest approach the bow shock was identified by an abrupt broadband burst of electrostatic turbulence at a radial distance of 23.5 Uranus radii. Once Voyager was inside the magnetosphere, strong whistler-mode hiss and chorus emissions were observed at radial distances less than about 8 Uranus radii, in the same region where the energetic particle instruments detected intense fluxes of energetic electrons. Various other plasma waves were also observed in this same region. At the ring plane crossing, the plasma wave instrument detected a large number of impulsive events that are interpreted as impacts of micrometer-sized dust particles on the spacecraft. The maximum impact rate was about 30 to 50 impacts per second, and the north-south thickness of the impact region was about 4000 kilometers.

THE VOYAGER 2 FLYBY OF URANUS on 24 January 1986 revealed that the planet has a large and unusual magnetosphere. Here we present an overview of the principal results from the plasma wave (PWS) instrument (*1*), beginning with the first detection of radio emissions from Uranus and ending with results obtained a few days after closest approach.

Radio emissions. Because radio emissions escaping from the magnetosphere were expected to provide the first clear indication of a planetary magnetic field (*2*), the detection of radio bursts was an important objective as Voyager approached Uranus. In contrast to the situation at Jupiter and Saturn, radio emissions were not observed until the spacecraft was close to the planet. The first clear radio emissions from Uranus were detected by the PWS instrument on 19 January 1986, only about 5 days before closest approach, at frequencies of 31.1 and 56.2 kHz (Fig. 1). At this time Voyager was at a radial distance of about 275 Uranus radii (R_U). The emission is strongest in the 31.1-kHz channel and is highly variable, with numerous sporadic bursts on time scales of seconds

D. A. Gurnett and W. S. Kurth, Department of Physics and Astronomy, University of Iowa, Iowa City, IA 52242.
F. L. Scarf, TRW Space and Technology Group, Redondo Beach, CA 90278.
R. L. Poynter, Jet Propulsion Laboratory, California Institute of Technology, Pasadena, CA 91109.

and minutes. Sporadic emissions of this type are apparently rare, because several days elapsed before another comparable radio burst was detected.

A second type of radio emission was detected a few days later, about 18 hours before closest approach. This radio emission has much smoother temporal variations and can be seen in the 4-day overview plot of Fig. 2 at 17.8, 31.1, and 56.2 kHz. The emission exceeded the receiver noise level at about 40 R_U on the inbound pass, reached maximum intensity near closest approach (at about 1800 spacecraft event time on 24 January), and dropped below the receiver noise level at about 40 R_U on the outbound pass. Similar radio emissions were also detected up to much higher frequencies (~800 kHz) by the planetary radio astronomy experiment (*3*). Because of the smooth spectrum and slow temporal variations, this radio emission appears to be similar to escaping continuum radiation at Earth (*4*).

A third type of radio emission was detected during the outbound pass on the nightside of Uranus. This radio emission is composed of numerous narrow bandwidth (a few percent) components centered around 5 kHz and can be seen in the 5.62-kHz channel on 25 and 26 January (Fig. 2). This narrowband emission varies sporadically on time scales as short as a few seconds and was detected on and off for about 6 days after closest approach. The frequency is well above the local electron plasma frequency. Therefore, the waves must be propagating in the free space electromagnetic mode. Although not as steady, the radiation has many similarities to the narrowband electromagnetic emissions at Jupiter and Saturn (*5–8*). The Jovian and Saturnian emissions are believed to be produced by mode conversion from electrostatic waves near the electron cyclotron frequency (*9*). If the emissions from Uranus are generated at a frequency near the electron cyclotron frequency, then on the basis of the magnetic field model provided by the MAG team (*10*) the source is located at a radial distance near the orbit of Miranda.

Upstream waves, bow shock, and magnetopause. The first clear evidence of upstream waves associated with the bow shock of Uranus occurred at 0550 spacecraft event time on 23 January, when a strong burst of electron plasma oscillations was detected in the 1.78-kHz channel (Fig. 3). These waves are produced by electrons escaping into the solar wind from the bow shock and are a well-known feature of the upstream solar wind at Earth, Jupiter, and Saturn (*6, 11, 12*). Electron plasma oscillations occurred on and off for about 1 day until the spacecraft finally crossed the bow shock at 0728 on 24 January, at a radial distance of about 23.5 R_U. The bow shock is easily identified in these data by the abrupt broadband burst of electrostatic turbulence from about 0728 to 0735 spacecraft event time. The location of the shock is consistent with the location identified by the MAG (*10*) and PLS (*13*) instruments. Although the solar wind density is unusually high, the overall characteristics of the electrostatic turbulence are similar to other planetary bow shocks (*7*). Plasma wave turbulence is believed to play an important part in energy dissipation in collisionless shocks.

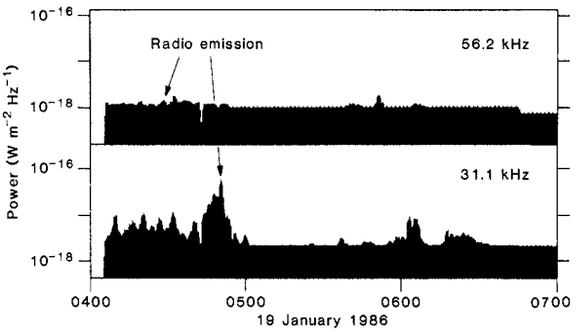

Fig. 1. The first radio emission from Uranus detected by Voyager 2. The instrument noise level is about 10^{-18} W m^{-2} Hz^{-1} (this threshold is somewhat uncertain because of a problem in the spacecraft data system). Horizontal scale designates spacecraft event time.

Downstream of the shock, the electric field intensities dropped to low levels throughout the magnetosheath, similar to the situation at Jupiter and Saturn. The MAG data show that the magnetopause, which marks the entry of Voyager 2 into the magnetosphere, occurred at 1007 (*10*). The only observable plasma wave effect at the magnetopause was a slight increase in the electric field intensities at 1.78 kHz. This increase is apparently due to electromagnetic radiation trapped in the low-density cavity formed by the magnetosphere, similar to the trapped continuum radiation at Jupiter (*12*).

Magnetosphere. After Voyager crossed the magnetopause, the plasma wave intensities remained relatively low until the spacecraft reached the inner region of the magnetosphere at radial distances less than about 8 R_U (Fig. 4). The inner magnetosphere is characterized by strong whistler-mode emissions that occur below the electron cyclotron frequency (f_c = 28 B Hz, where B is the magnetic field strength) and extend almost continuously from about 1520 on the inbound pass, through the region near closest approach, to about 2110 on the outbound pass. These waves were identified as whistler-mode emissions on the basis of the

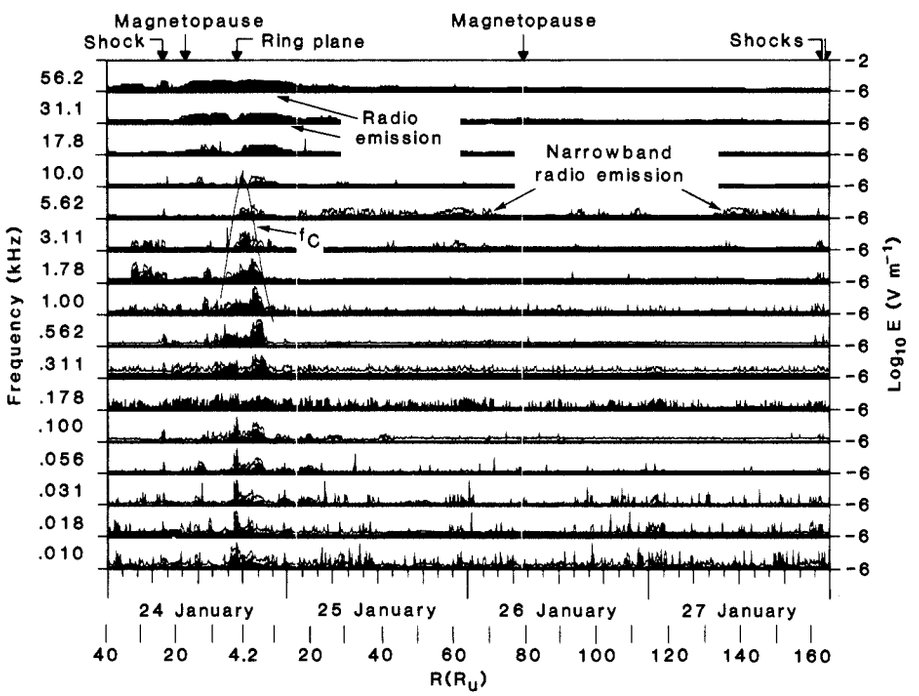

Fig. 2. A 16-channel overview plot of the electric field (E) intensities from the PWS instrument. This 4-day plot covers the period from shortly before the inbound shock crossing to shortly after the first outbound shock crossing. The solid line labeled f_c gives the electron cyclotron frequency, computed from a model provided by Ness and colleagues (*10*).

frequency range, which is always below the electron cyclotron frequency, and comparisons to similar broadband spectrograms at Earth, Jupiter, and Saturn. To illustrate these comparisons, we obtained six 10-second spectrograms of the broadband data which are shown in Fig. 5. These spectrograms were obtained from short segments of the electric field waveform that were digitized at a high rate (28,800 samples per second) on the spacecraft, transmitted to the ground, and then Fourier-transformed to produce spectrograms. Spectrograms A, B, C, and F in Fig. 5 show a type of whistler-mode emission known as hiss. Whistler-mode hiss has relatively little spectral structure and occurs in the plasmasphere at Earth, in Io's plasma torus at Jupiter, and in the magnetosphere of Saturn (*6, 12, 14*). Figure 5B shows another type of whistler-mode emission known as chorus. Chorus consists of many discrete tones, usually rising in frequency with increasing time, and also occurs in the magnetospheres of Earth, Jupiter, and Saturn (*6, 15*).

Chorus and hiss are both believed to be produced by cyclotron resonance interactions with energetic electrons. The free energy source comes from the anisotropy produced by the loss cone in the distribution of trapped electrons. For many years whistler-mode emissions have been thought to play an important role in planetary radiation belts because they cause pitch angle scattering, eventually precipitating the particles into the atmosphere. Because the wave intensities increase rapidly as the number of resonant particles increases, this loss mechanism limits the maximum electron flux in the radiation belt (*16*). The electron precipitation into the atmosphere can also produce auroral light emissions.

It is useful to estimate the resonance energies for the whistler-mode emissions observed in the magnetosphere of Uranus. For the chorus emissions in Fig. 5B (at 1802, the electron resonance energy for parallel propagation is about 240 keV if an electron density of about 0.4 cm^{-3} is assumed. This electron density is based on initial estimates from the PLS instrument (*13*). For the hiss in Fig. 5F (at 2035), the electron resonance energy is about 60 keV if an electron density of 0.3 cm^{-3} is assumed. In both cases the resonance energies are in a region of the energy spectrum where the LECP instrument detected intense fluxes of trapped electrons (*17*). These electrons presumably provide the free energy source for the waves. The hiss emission became particularly intense on the outbound pass near 2000 (Fig. 4), with maximum broadband electric field amplitudes of 1.9 mV m^{-1}. The reason for the intensification in this region is not known because comparable intensities were not observed on the same L shells on the inbound pass. In any case, the large wave intensities should produce rapid pitch angle scattering and precipitation of trapped electrons, thereby possibly accounting for the ultraviolet emissions observed on the nightside of Uranus (*18*).

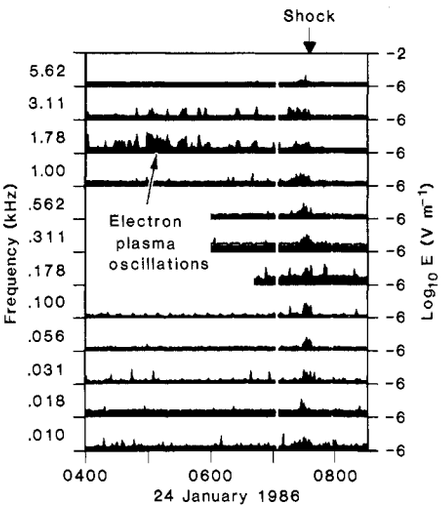

Fig. 3. An expanded-scale plot of Fig. 2 showing upstream electron plasma oscillations and the burst of plasma wave turbulence at the inbound shock crossing. Horizontal scale designates spacecraft event time.

In addition to the whistler-mode emissions, various other plasma waves were observed in the inner magnetosphere. On the inbound pass, strong emissions can be seen in the 1.00- and 1.78-kHz channels from about 1240 to 1320 (Fig. 2), slightly above the electron cyclotron frequency. These emissions are almost certainly electrostatic $3f_c/2$ electron cyclotron waves, similar to the electrostatic electron cyclotron waves observed at Earth, Jupiter, and Saturn (*6, 12, 19*). Two other unusual types of emissions can be seen at frequencies from a few hundred hertz to about 1 kHz in Fig. 5, D and E (at 1920 and 1947). Inspection of the 16-channel plot in Fig. 4 shows that the entire region from about 1910 to 1930 has many intense bursts similar to those in Fig. 5D. This region is also remarkably devoid of whistler-mode hiss. We have no clear identification of the plasma wave mode responsible for these bursts. Comparison with the MAG (*10*) and LECP (*17*) data suggests that this region may be associated with Miranda's L shell.

The outbound pass through the magnetotail was characterized by low plasma wave intensities. The only clearly identifiable plasma wave emissions were at frequencies below 100 Hz from about 0130 to 0330 on 25 January (Fig. 2). The outbound magnetopause crossing was also characterized by low

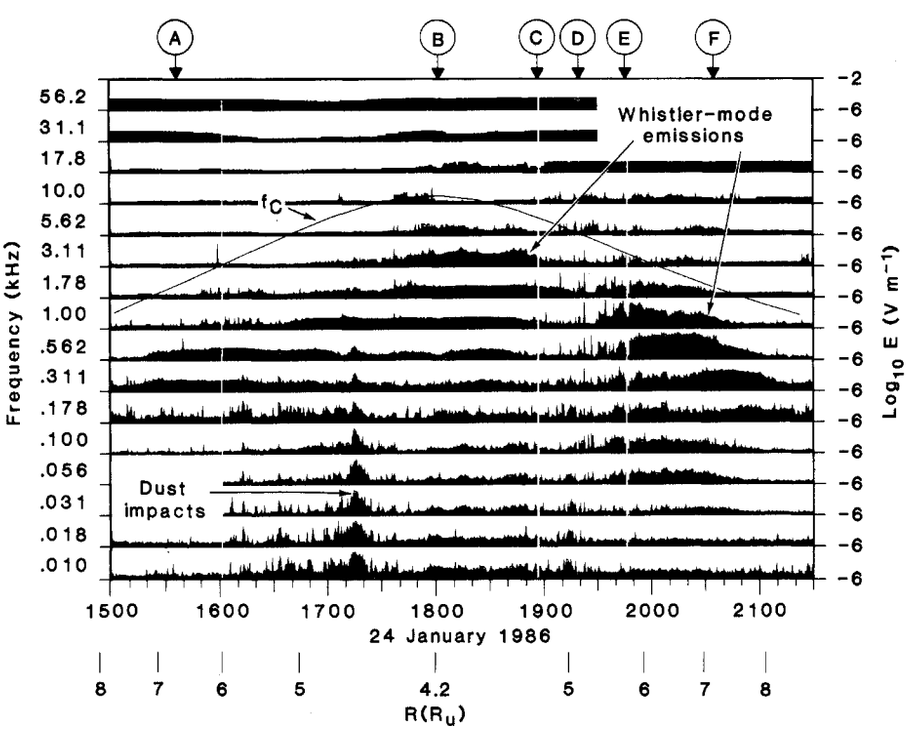

Fig. 4. A 16-channel plot showing the electric field (E) intensities in the inner region of the magnetosphere. The broad region of noise below the electron cyclotron frequency [f_c, solid line (*10*)] is caused by whistler-mode emissions. The intense burst of low-frequency noise at about 1715 spacecraft event time is caused by dust impacts. The circled letters at the top correspond to spectra in Fig. 5.

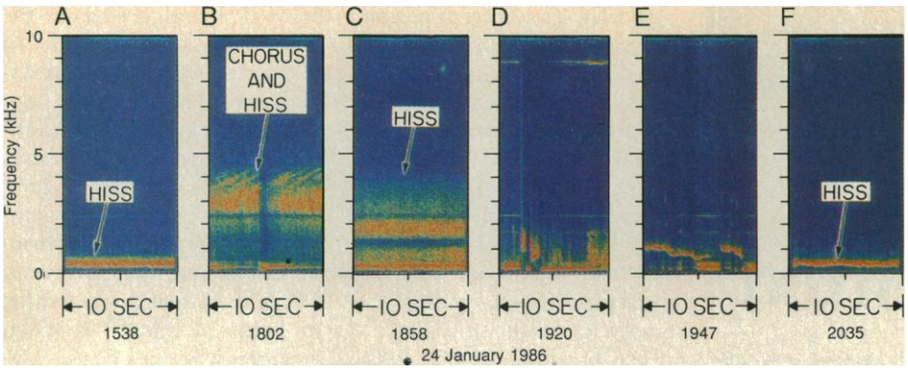

Fig. 5. A series of broadband frequency-time spectrograms for selected regions in Fig. 4. Hiss and chorus are both whistler-mode emissions. The plasma wave mode responsible for the emissions in (D) and (E) has not been identified.

intensities. Several bow shock crossings were observed during the outbound pass, all with characteristics similar to those shown in Fig. 3. After Voyager exited the magnetosphere, sporadic bursts of electron plasma oscillations were observed in the solar wind for a period of several weeks. These waves are believed to be caused by electrons streaming outward, away from the shock, along the interplanetary magnetic field.

Ring plane. As the spacecraft passed through the ring plane at about 1715 on 24 January, an intense burst of low-frequency noise coincided almost exactly with the time of the ring plane crossing. This noise, which lasted about 6 minutes, can be seen in Fig. 4 at frequencies below about 1 kHz, increasing in intensity with decreasing frequency. The characteristics of this noise are similar to the noise observed during the Voyager 2 ring plane crossing at Saturn, when many micrometer-sized dust particles struck the spacecraft (*8, 20*). Investigation of the broadband data at the Uranus ring plane confirms that the noise is caused by dust impacts. The waveform from the broadband receiver (Fig. 6) consists of impulses lasting a few milliseconds and is similar to that for the dust impacts at Saturn. At the time of maximum intensity, around 1715:30, the impact rate is about 30 to 50 impacts per second as judged from initial estimates.

As presently understood, the impulsive voltage produced by a dust impact is caused by the charge released when a particle strikes the spacecraft. Laboratory measurements (*21*) show that when a small particle strikes a solid surface at a high velocity the particle is instantly vaporized and ionized, producing a small cloud of plasma that expands away

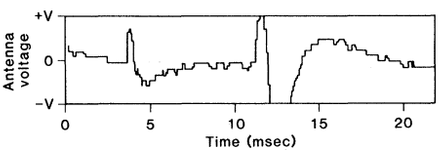

Fig. 6. A voltage waveform from the broadband receiver, showing two dust impacts detected near the ring plane crossing (1716 spacecraft event time on 24 January).

from the impact site. As the plasma cloud sweeps over the electric antenna, some of the charge is collected by the antenna, thereby causing a voltage pulse. Laboratory measurements show that the charge released is directly proportional to the mass of the particle. The pulse amplitude is therefore proportional to the mass.

Because Voyager 2 passed through the ring plane at about 4.5 R_U, well beyond the visible rings, the dust impacts detected by the PWS instrument are not directly associated with the rings. It is possible, of course, that these dust particles may represent a disklike extension of the visible ring system out to where Voyager crossed the ring plane. Miranda could be another possible source. As judged from the similarity to the dust impacts at Saturn, the impacts at Uranus are probably caused by particles in the micrometer size range. The number density, n, can be estimated from the relation $R = nUA$, where R is the counting rate, U is the spacecraft speed, and A is the area of the spacecraft. From nominal values, the maximum number density is about 10^{-3} particles per cubic meter. From the duration we estimate the north-south thickness, L, of the dust impact region to be about 4000 km. The columnar number density, nL, is then on the order of a few thousand particles per square meter. For micrometer-sized particles this number density is too small to be detected with the imaging system.

REFERENCES AND NOTES

1. For a description of the PWS instrument, see F. L. Scarf and D. A. Gurnett, *Space Sci. Rev.* **21**, 289 (1977).
2. Possible magnetospheric radio emissions from Uranus were reported by L. W. Brown [*Astrophys. J.* **207**, L209 (1976)], who used data from an earth-orbiting spacecraft.
3. J. W. Warwick *et al.*, *Science* **233**, 102 (1986).
4. D. A. Gurnett, *J. Geophys. Res.* **80**, 2751 (1975); W. S. Kurth, D. A. Gurnett, R. R. Anderson, *ibid.* **86**, 5519 (1981).
5. J. W. Warwick *et al.*, *Science* **204**, 995 (1979).
6. D. A. Gurnett, W. S. Kurth, F. L. Scarf, *ibid.* **212**, 235 (1981).
7. ———, *Nature (London)* **292**, 733 (1981).
8. F. L. Scarf *et al.*, *Science* **215**, 587 (1982).
9. D. A. Gurnett and L. A. Frank, *J. Geophys. Res.* **81**, 3875 (1976); D. Jones, *Nature (London)* **260**, 686 (1976); D. B. Melrose, *J. Geophys. Res.* **86**, 30 (1981).
10. N. F. Ness *et al.*, *Science* **233**, 85 (1986).
11. F. L. Scarf *et al.*, *J. Geophys. Res.* **76**, 5162 (1971).
12. F. L. Scarf, D. A. Gurnett, W. S. Kurth, *Science* **204**, 991 (1979).
13. H. S. Bridge *et al.*, *ibid*, **233**, 89 (1986).
14. R. M. Thorne *et al.*, *J. Geophys. Res.* **78**, 1581 (1973).
15. R. A. Helliwell, *Whistlers and Related Ionospheric Phenomena* (Stanford Univ. Press, Stanford, CA, 1965), p. 207; F. F. Coroniti *et al.*, *Geophys. Res. Lett.* **7**, 45 (1980).
16. C. F. Kennel and H. E. Petschek, *J. Geophys. Res.* **71**, 1 (1966).
17. S. M. Krimigis *et al.*, *Science* **233**, 97 (1986).
18. A. L. Broadfoot *et al.*, *ibid.*, p. 74.
19. C. F. Kennel *et al.*, *J. Geophys. Res.* **75**, 6136 (1970).
20. D. A. Gurnett *et al.*, *Icarus* **53**, 236 (1983).
21. H. Fechtig, E. Grün, J. Kissel, in *Cosmic Dust*, J. A. M. McDonnell, Ed. (Wiley, New York, 1978), p. 607.

22. We thank the Voyager team at the Jet Propulsion Laboratory and the staff at NASA Headquarters for their valuable support; E. Miner for his efforts in scheduling the broadband coverage and J. Anderson, C. Avis, and the staff of the Multimission Image Processing Laboratory for their assistance with the broadband data processing; N. Toy and the General Science Data Team for timely and efficient production of quick-look data products; the Planetary Data System for the use of its facilities; the Space Physics Analysis Network for the use of its facilities in communicating data between the University of Iowa and the Jet Propulsion Laboratory; S. Chang, K. Jordan, R. Brechwald, L. Granroth, J. Cook-Granroth, and R. Kraemer for programming support; N. Ness, S. M. Krimigis, H. Bridge, and J. Warwick for their helpful discussions and data comparisons. We also remember C. Stembridge for his dedication to the excellence of the Voyager mission and his continual support of the PWS investigation. The research at the University of Iowa was supported by NASA through contract 954013 with the Jet Propulsion Laboratory, by grants NGL-16-001-043 and NGL-16-001-002 with NASA Headquarters, by the Office of Naval Research through contract N00014-85-K-0404, and by the State of Iowa through a faculty development assignment (to D.A.G.). The research at TRW was supported by NASA through contract 954012 with the Jet Propulsion Laboratory.

31 March 1986, accepted 5 May 1986